The Role of Copper in Topa Quinone Biogenesis and Catalysis, as Probed by Azide Inhibition of a Copper Amine Oxidase from Yeast†

Benjamin Schwartz, Amy K. Olgin, and Judith P. Klinman*

Departments of Chemistry and of Molecular and Cell Biology, University of California, Berkeley, California 94720

Received September 11, 2000; Revised Manuscript Received December 14, 2000

ABSTRACT: All known copper amine oxidases (CAOs) contain 2,4,5-trihydroxyphenylalanine quinone (TPQ) as a redox cofactor. TPQ is derived posttranslationally from a specific tyrosine residue within the protein itself, and is utilized by the enzyme to oxidize amines to aldehydes. Several oxidative mechanisms for both turnover and the biogenesis of the cofactor have been proposed in recent years, which differ mainly in the nature of the interaction of oxygen with the enzyme. In this study, azide is used to probe the role of copper in catalysis and biogenesis, especially with respect to potential interactions between the metal and oxygen. During turnover, it is found that azide is a noncompetitive inhibitor with respect to O_2, most consistent mechanistically with oxygen binding off the metal prior to reaction. During biogenesis, it is found that azide likely prohibits ligation of the precursor tyrosine to the copper, thus preventing the formation of this key intermediate. This result is consistent with previous proposals, where the copper−tyrosine unit is the species that undergoes reaction with O_2. In addition, it is found that oxygen consumption is kinetically uncoupled from TPQ formation; this leads to an expanded kinetic model for biogenesis, with important implications for previous results.

Copper amine oxidases (CAOs)[1] catalyze the two-electron, oxidative deamination of amines, utilizing molecular oxygen as the terminal electron acceptor:

$$RCH_2NH_3^+ + O_2 + H_2O \rightarrow RCHO + NH_4^+ + H_2O_2 \quad (1)$$

To accomplish this reaction, all known CAOs contain a novel redox cofactor, 2,4,5-trihydroxyphenylalanine quinone (TOPA quinone or TPQ) (Figure 1) (*1*). TPQ is not dissociable from its cognate enzyme, due to its derivation from a specific tyrosine residue within the protein itself (*2*). This process, referred to as biogenesis, occurs in an autocatalytic manner, without the requirement for accessory proteins or cofactors (*3*, *4*). Thus, CAOs are able to catalyze both the oxidation of amines and the initial oxygenation of tyrosine within a single active site.

Structural data have been obtained for the mature, TPQ-containing protein from several sources, including *Escherichia coli* (ECAO), pea seedling (PSAO), *Arthrobacter globiformis* (AGAO), and *Hansenula polymorpha* (HPAO)

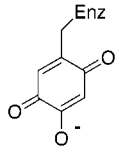

TPQ

FIGURE 1: Structure of 2,4,5-trihydroxyphenylalanine quinone, or TPQ.

(*5*−*9*). Two structures have also been obtained for the apo form of the enzyme, one without metal (*8*) and one containing zinc in the active site (*10*). These have contributed greatly toward our understanding of both catalysis and biogenesis, particularly as analogues of intermediates in both processes have been observed crystallographically (*10*, *11*).

Detailed spectroscopic and kinetic analyses have also been conducted for catalysis (*12*−*19*), and to a lesser extent for biogenesis (*20*−*23*). Overall, an explicit mechanistic picture has been developed for catalysis (Scheme 1) that is supported by an abundance of experimental evidence. Our understanding of biogenesis is less well developed, but is beginning to converge toward plausible proposals.

An important aspect of both mechanisms, which has remained poorly defined, is the nature of the interaction between the enzyme and molecular oxygen. During catalysis, it has been proposed that the cofactor is either oxidized directly by O_2 (Scheme 2A), or oxidized indirectly via the active site copper (Scheme 2B). In the first scenario, oxygen is bound in a nonmetal site prior to reaction with reduced cofactor, whereas in the second proposal oxygen reacts directly with Cu^{1+}. Evidence for the latter proposal consists of direct observation of the Cu^{1+}−semiquinone species

† This work was supported by a grant from the NIH (GM 39296) to J.P.K. B.S. was supported by a postdoctoral grant from the NIH (GM 18813). A.K.O. was supported by a McNair undergraduate scholarship.

* To whom correspondence should be addressed. Email: klinman@socrates.berkeley.edu; Tel: (510) 642-2668; Fax: (510) 643-6232.

[1] Abbreviations: CAOs, copper-containing amine oxidases; TPQ, 2,4,5-trihydroxyphenylalanine quinone; ECAO, *Escherichia coli* amine oxidase; PSAO, pea seedling amine oxidase; AGAO, *Arthrobacter globiformis* amine oxidase; HPAO, *Hansenula polymorpha* amine oxidase; BSAO, bovine serum amine oxidase; PPAO, porcine plasma amine oxidase; apo-HPAO, metal-free, TPQ-free enzyme; apo-Cu HPAO, metal-containing, TPQ-free enzyme; holo-HPAO, metal-containing, TPQ-containing enzyme; LMCT band, ligand to metal charge-transfer band.

10.1021/bi0021378 CCC: $20.00
Published on Web 02/10/2001

Scheme 1: Catalytic Mechanism for Copper Amine Oxidases

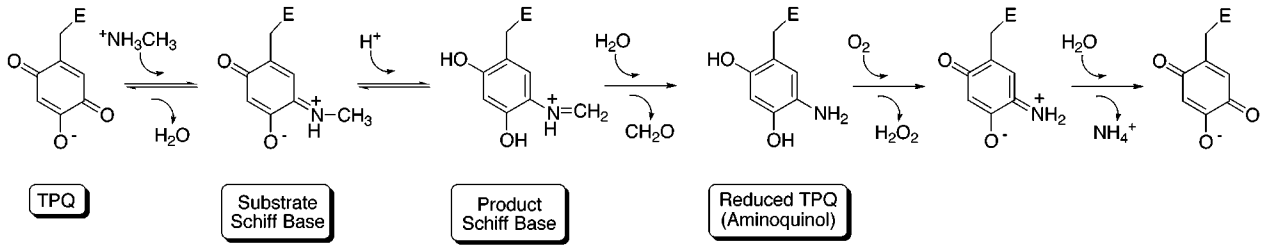

Scheme 2: Proposed Mechanisms for the Catalytic Oxidative Half-Reaction

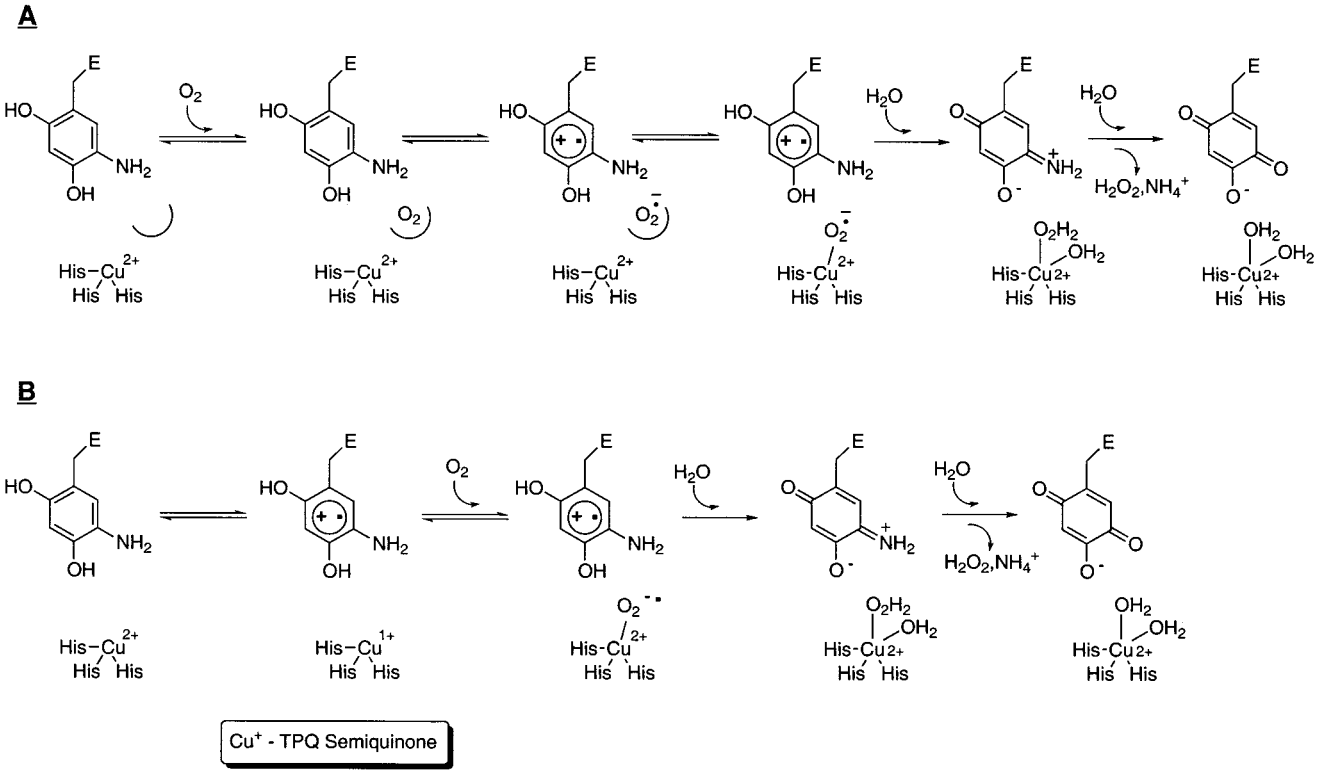

(Scheme 2B) by EPR experiments in anaerobic, substrate-reduced enzyme from various sources (*18*). In addition, it has been shown that the Cu^{1+}−semiquinone can form from reduced cofactor at a catalytically competent rate (*24*). Support for the former hypothesis includes extensive kinetic experiments with bovine serum amine oxidase (BSAO) and HPAO, as well as metal replacement studies in HPAO (*16*, *25*). These latter experiments suggest that single electron transfer from reduced cofactor to metal occurs off the reaction pathway.

Analogous to the proposals for catalysis, it has been suggested either that O_2 prebinds to CAOs in a nonmetal site (*23*), or that it reacts directly with reduced copper (*8*) during biogenesis. However, in contrast to catalytic turnover, much less data exist addressing key intermediates in the biogenetic process.

Azide has previously been shown to be a ligand for copper in several mature CAOs (*26*−*30*). To understand further the interaction between O_2 and the enzyme, this study explores the effect of azide on the oxidative chemistry of HPAO. During catalysis, N_3^- is found to be a noncompetitive inhibitor with respect to O_2, consistent with oxygen binding to a nonmetal site prior to reaction. During biogenesis, N_3^- appears to inhibit formation of the precursor tyrosine−copper complex, a crucial intermediate in initiating TPQ formation. Detailed kinetic analysis, with and without N_3^-, once again supports a mechanism in which O_2 binds initially to HPAO off of the metal. The implications of these results are discussed, and are compared with previous investigations of amine oxidases.

MATERIALS AND METHODS

Metal-free apo-HPAO was prepared as previously described (*31*). Sodium azide was purchased from Sigma-Aldrich and used without further purification. $CuCl_2$ (Aldrich) was used as the source of Cu^{2+}. Inhibition data for catalysis were fitted using the KINETICS program (*32*). Biogenesis simulations were conducted using an SGI version of the KINSIM program.

Azide Inhibition Studies of Turnover. CAO activity was monitored by measuring the rates of oxygen consumption on a Clark electrode (YSI model 5300) at 25 °C as previously described (*17*). The concentration of oxygen was varied by blowing a mixture of N_2 and O_2 over the 1 mL solution for a minimum of 10 min to allow for equilibration. Assays were conducted in 100 mM potassium phosphate (total ionic strength = 300 mM), with 3 mM methylamine (MeAm) (*17*) and various concentrations of NaN_3, depending on pH (0−

100 mM at pH 6.0, 0−200 mM at pH 7.0, and 0−500 mM at pH 8.0).

To ensure that the observed effects of azide on enzyme activity were due to inhibition of the oxidative, and not reductive, half-reaction, the K_M for amine was determined at the highest concentration of N_3^- used (500 mM). This control revealed that with no N_3^- present the K_M for methylamine was equal to 0.129 mM, while at high N_3^- the $K_M = 0.349$ mM. Though there is a small effect, the values for K_M (both with and without azide) are well below the concentration of substrate used in measuring k_{cat}/K_M for oxygen (3 mM MeAm), and thus the effects of N_3^- can be confidently correlated with the oxidative half-reaction.

The effect of ionic strength was studied by comparing $k_{cat}/K_M(O_2)$ in a control reaction (without NaN_3) to that of a reaction containing 800 mM potassium phosphate; no effect was observed due to increased ionic strength under these conditions. Finally, since assays were initiated by adding enzyme to a reaction containing all elements (including azide), it was necessary to ensure that azide bound rapidly to HPAO. The enzyme was preincubated with azide for various times (0−15 min), and MeAm used to initiate catalysis. No differences were found in these reactions.

Titration of Apo-HPAO and Holo-HPAO with Azide. Azide titrations were followed on an HP8452A diode-array spectrophotometer (Hewlett-Packard), fitted with a constant-temperature bath. For anaerobic titrations of apo-Cu HPAO, a hand-crafted cuvette with a bulbous top and ground glass joint was used, and the enzyme preparation was first made anaerobic by passing a stream of pyrogallol-scrubbed argon over the sample for 1 h, as previously described (*17*). Following this, a solution of copper (1 mM) was sparged with argon for 30 min, and then 6 μL (40 μM) was added to an anaerobic preparation of HPAO (40 μM, 150 μL). After no further spectral changes were observed (*22*), aliquots of an anaerobic azide solution were added via a gastight syringe, and the absorbance at 410 nm was recorded. Titrations of holo-HPAO were conducted aerobically, with sequential additions of azide to mature enzyme.

UV−Vis Spectroscopic Biogenesis Experiments. TPQ formation was initiated either by the introduction of oxygen to an anaerobic solution of apo-HPAO with copper prebound in the absence of O_2, or by the addition of copper to an aerobic solution of apo-HPAO; both of these procedures have been described previously (*23*). These reactions contained 40 μM apo-HPAO, in 150 μL of total buffer. Reactions varied in azide content, from 0 to 10 mM total concentration. To avoid azide-mediated photodamage of apo-HPAO, a minimum number of spectra were recorded (30 per experiment).

Experiments varying in oxygen were conducted in a sealed cuvette, similarly to anaerobic experiments, but using a stream consisting of a mixture of N_2 and O_2. For each spectroscopic experiment, the mixture of N_2 and O_2 was also passed over a buffered solution in an oxygen electrode to accurately determine the concentration of O_2.

To observe the 350 nm biogenesis intermediate without attendant photodamage in the presence of various concentrations of azide, a single-wavelength spectrophotometer (CARY Instruments, 3 BIO) was used.

Biogenesis Experiments on the Oxygen Electrode. Oxygen consumption during biogenesis was monitored with a Clark oxygen electrode (YSI model 5300). Apo-HPAO (10 μM, 1 mL) was equilibrated with varying concentrations of azide (0−10 mM) until a stable baseline was achieved. One equivalent of copper was then added to initiate biogenesis. The full reaction was fit to a single exponential to calculate k_{obs} (*23*).

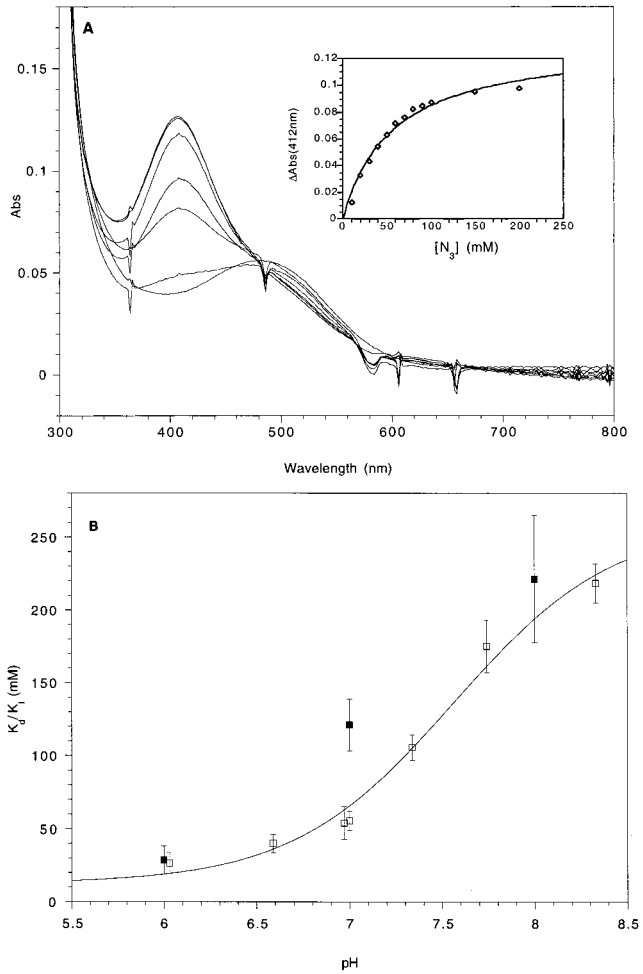

FIGURE 2: (A) Spectral changes accompanying titration of holo-HPAO with azide at pH 7.0. Absorbance changes at 412 nm were fit to a titration curve (inset), with a resulting K_d of 55.5 mM. (B) pH dependence of K_d (□) for holo-HPAO and of K_I for $k_{cat}/K_M(O_2)$ (■) for azide. K_I values were calculated using a kinetics program by Cleland (*32*).

RESULTS

Titration of Holo-HPAO with Azide. Mature HPAO was titrated by the addition of sequential aliquots of sodium azide. Changes in absorbance were observed at 408 nm (Figure 2A); from these spectral changes, a dissociation constant of 55.5 mM (inset) and an ϵ value of 1.4×10^3 M^{-1} cm^{-1} were calculated. Titrations were carried out over a pH range of 6.0−8.2 (Figure 2B); K_d decreased at lower pHs, and the data were fit to a model for two limiting values (low and high pH), controlled by a single pK_a:

$$K_d = K_{d(\text{low pH})}/[1 + 10^{(\text{pH}-\text{p}K)}] + K_{d(\text{high pH})}/[1 + 10^{(\text{p}K-\text{pH})}]$$

Values of 12.5 (±9.6) mM and 260 (±18) mM were calculated for K_d at low and high pHs, respectively, with a pK_a of 7.56 (±0.11).

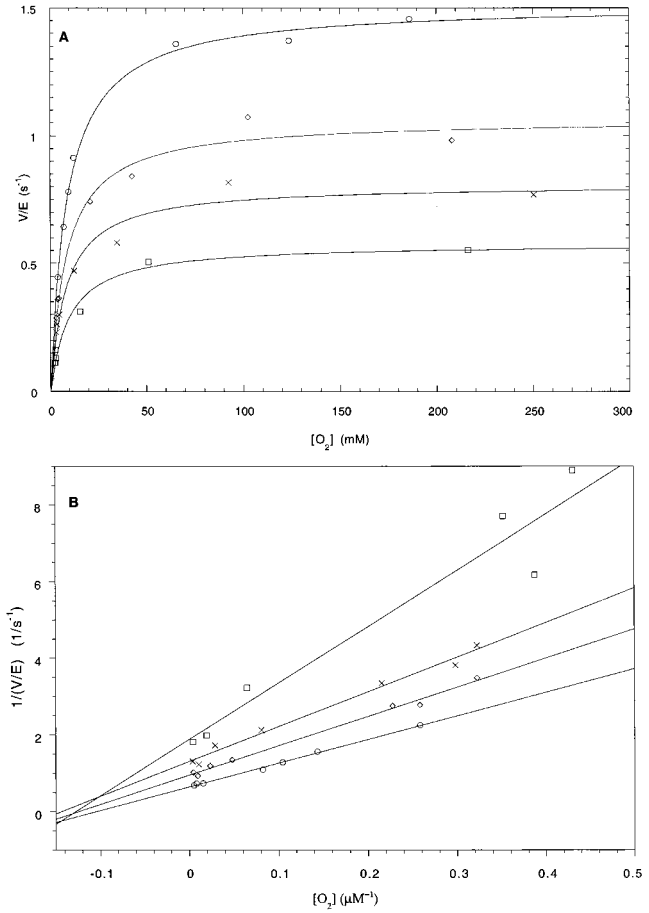

FIGURE 3: (A) Michaelis−Menten plots of initial rates vs $[O_2]$ during catalysis in the presence of 0 (○), 50 mM (◇), 100 mM (×), and 200 mM (□) NaN_3. (B) Lineweaver−Burke plots demonstrating the noncompetitive inhibition mode of azide. Concentrations of NaN_3 are the same as in panel A.

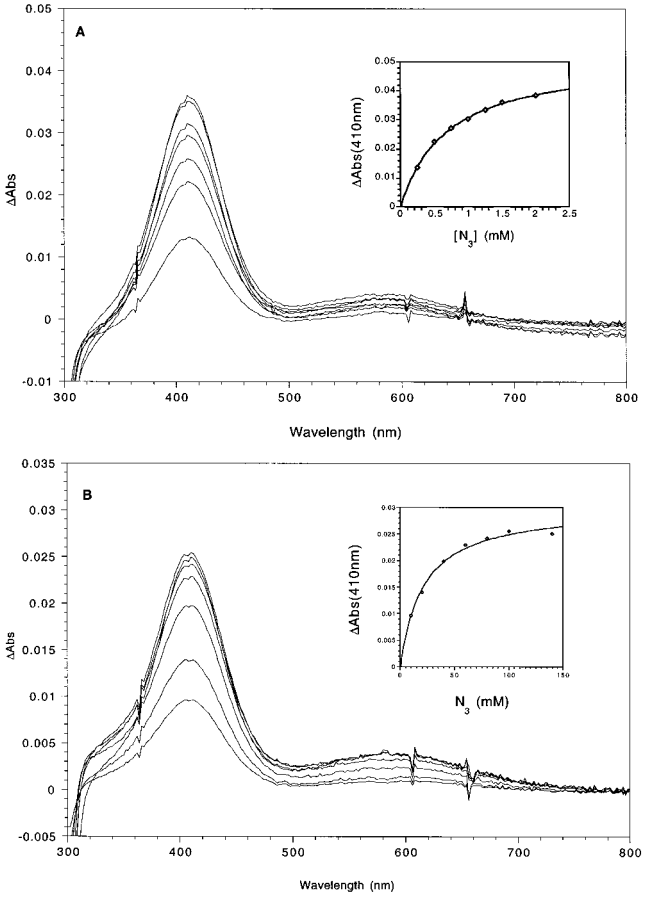

FIGURE 4: (A) Spectral changes accompanying the first titration of apo-Cu HPAO with azide. Absorbance changes at 408 nm were fit to a titration curve (inset), with a resulting K_d of 0.67 mM. (B) Spectral changes accompanying the second titration of apo-Cu HPAO with azide. Absorbance changes at 410 nm were fit to a titration curve (inset), with a resulting K_d of 21.1 mM.

Inhibition of $k_{cat}/K_M(O_2)$ by Azide. Azide was found to inhibit the oxidative half-reaction (Figure 3A,B) in a manner consistent with noncompetitive inhibition. This pattern was found to be independent of pH, even though the K_I for azide is affected; the K_I was found to be roughly equal to the K_d determined by titration (Figure 2B).

To assess whether azide inhibition was time-dependent, inhibition of activity was measured after preincubating enzyme with NaN_3 for various times (0−15 min). No effect was observed, consistent with the spectroscopic observation of rapid binding (>1 s^{-1}).

Titration of Anaerobic, Copper-Containing Precursor HPAO (Apo-Cu HPAO) with Azide. Anaerobic apo-Cu HPAO (50 mM HEPES, pH 7.0) was titrated with aliquots (0.25 mM) of anaerobic NaN_3, and absorbance changes at 412 nm were observed (Figure 4A); based on this, a K_d for azide of 0.67 mM (inset) and an ϵ value of 9.6×10^2 M^{-1} cm^{-1} were calculated. Absorbance changes at concentrations of azide greater than 1.5 mM and less than 5 mM were not found. However, subsequent additions of 10−20 mM aliquots of azide led to the observation of a second titration of apo-Cu HPAO (Figure 4B). A second K_d for azide of 21.1 mM and an ϵ value of 6.3×10^2 M^{-1} cm^{-1} were calculated based on the observed absorbency changes at 410 nm (inset).

Spectral Changes during Biogenesis with and without Azide. Initiation of biogenesis with oxygen to a solution of apo-Cu HPAO led to the time-dependent spectral changes shown in Figure 5A. A similar experiment conducted in the presence of 2 mM NaN_3 is shown in Figure 5B; initially a peak due to azide (410 nm) is observed, and upon addition of oxygen, the peak decreases isosbestic with the formation of TPQ (480 nm).

Effect of Azide on Accumulation of the Biogenesis Intermediate. Biogenesis was initiated as above, but followed at 350 and 480 nm using a single-wavelength spectrophotometer (3 BIO, CARY Instruments) to minimize azide-mediated photodamage. The accumulation of the 350 nm intermediate was sensitive to the concentration of azide (Figure 6) at concentrations proximal to the first K_d for N_3.

Effect of Azide on k_{obs} for O_2 Depletion and TPQ Formation. The observed rates of oxygen consumption and TPQ formation were studied as a function of azide concentration (Figure 7). As N_3^- concentration increases, both rates decrease but become closer in value.

Effect of Oxygen Concentration on k_{obs} for O_2 Depletion and TPQ Formation. The observed rates of oxygen consumption and TPQ formation were studied as a function of oxygen concentration (Figure 8). As the concentration of O_2 increases, k_{obs} for TPQ saturates at relatively low $[O_2]$ (200 μM), while k_{obs} for the consumption of oxygen shows minimal saturation up to maximally obtainable values (1 mM).

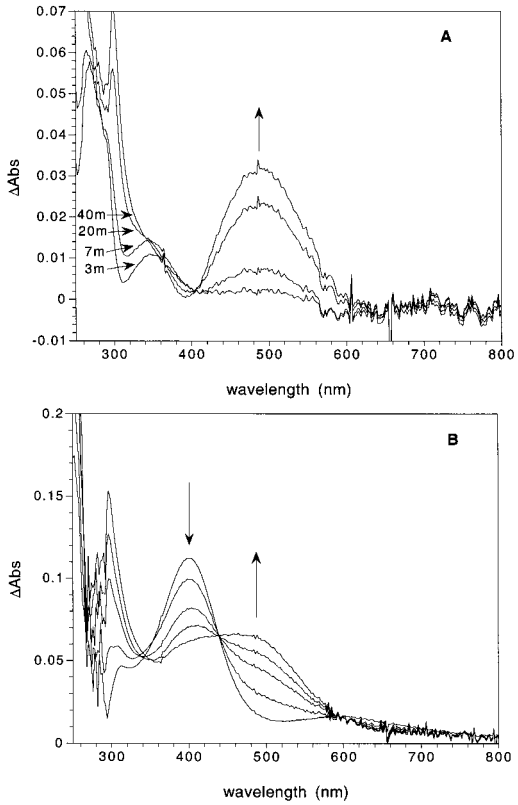

FIGURE 5: (A) Spectral changes accompanying biogenesis, in the absence of azide, relative to anaerobic apo-Cu HPAO. The spectra shown are the changes in absorbance following the introduction of oxygen at 3, 7, 20, and 40 min (*22*). (B) Spectral changes accompanying biogenesis, in the presence of 2 mM NaN_3, relative to anaerobic apo-Cu HPAO. The spectra shown represent the changes in absorbance at 3, 15, 30, 45, and 72 min after the introduction of oxygen.

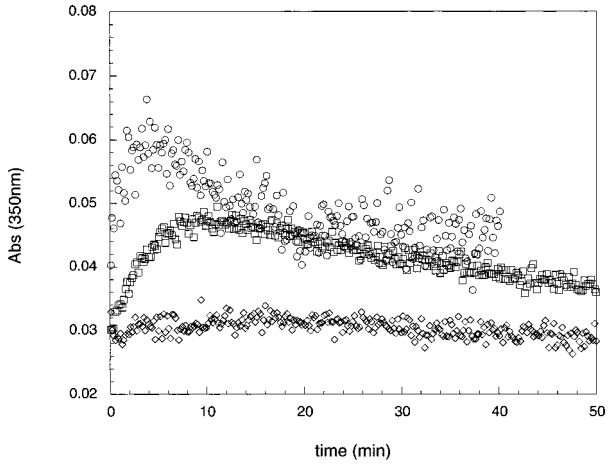

FIGURE 6: Effect of azide concentration on the accumulation of the 350 nm species during biogenesis. The 350 nm intermediate was observed during biogenesis without azide (○), or in the presence of 1 mM NaN_3 (□) or 5 mM NaN_3 (◇).

DISCUSSION

CAOs are a class of enzymes found in bacteria, yeast, plants, and mammals, that catalyze the oxidative deamination of amines (*33*). Though the biological functions of these enzymes are still not well-defined for many organisms, there does exist general agreement about many mechanistic aspects. All CAOs contain TPQ as a redox cofactor for catalysis, and form TPQ in an autocatalytic, posttranslational

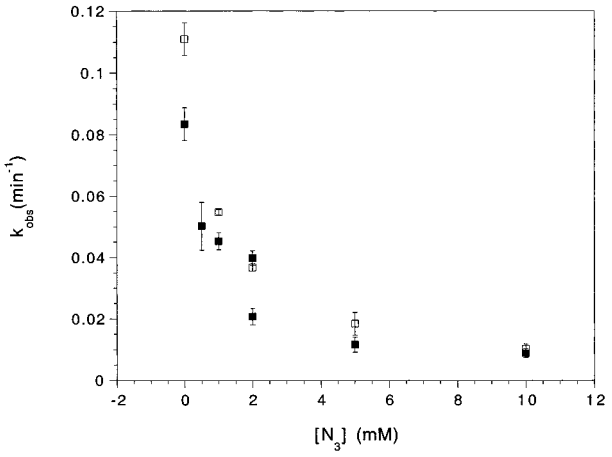

FIGURE 7: Effect of azide on k_{obs} for O_2 consumption (□) and TPQ formation (■) during biogenesis.

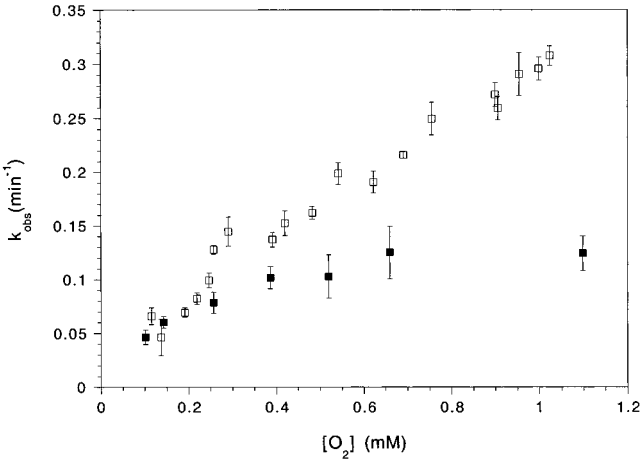

FIGURE 8: Effect of oxygen concentration on k_{obs} for O_2 consumption (□) and TPQ formation (■) during biogenesis.

process from a specific tyrosine residue within the protein itself. During catalysis, substrate amines are activated via formation of a series of Schiff base complexes with TPQ (Scheme 1) in the reductive half-reaction, followed by cofactor reoxidation to regenerate resting enzyme. During biogenesis, the precursor tyrosine is proposed to ligand the active site copper (C in Scheme 3) as the initializing step.

Support for the mechanisms shown in Schemes 1 and 3 comes from a range of crystallographic, spectroscopic, and kinetic probes over the past decade (*5*−*25*). However, there remains a lack of consensus surrounding the specific details of the oxidative chemistries of both catalysis and biogenesis. During catalysis, a direct reaction between O_2 and reduced active site copper (Scheme 2B) had been proposed, based on EPR experiments where appreciable Cu^{+}−TPQ semiquinone formation was directly observed in anaerobically, substrate-reduced amine oxidases from various sources (*18*). In contrast, a detailed kinetic analysis of BSAO, that included O-18 kinetic isotope effects, indicated that O_2 binds at a nonmetal site, and undergoes direct reaction with reduced TPQ cofactor (Scheme 2A) (*16*). This result is supported by recent metal replacement studies in HPAO, where protein-containing cobalt is found to support catalysis at a rate identical to the copper-containing enzyme (*25*).

During biogenesis, recent spectroscopic and kinetic investigation indicated that oxygen is likely prebound at a

Scheme 3: Previous Biogenesis Proposal (*23*)

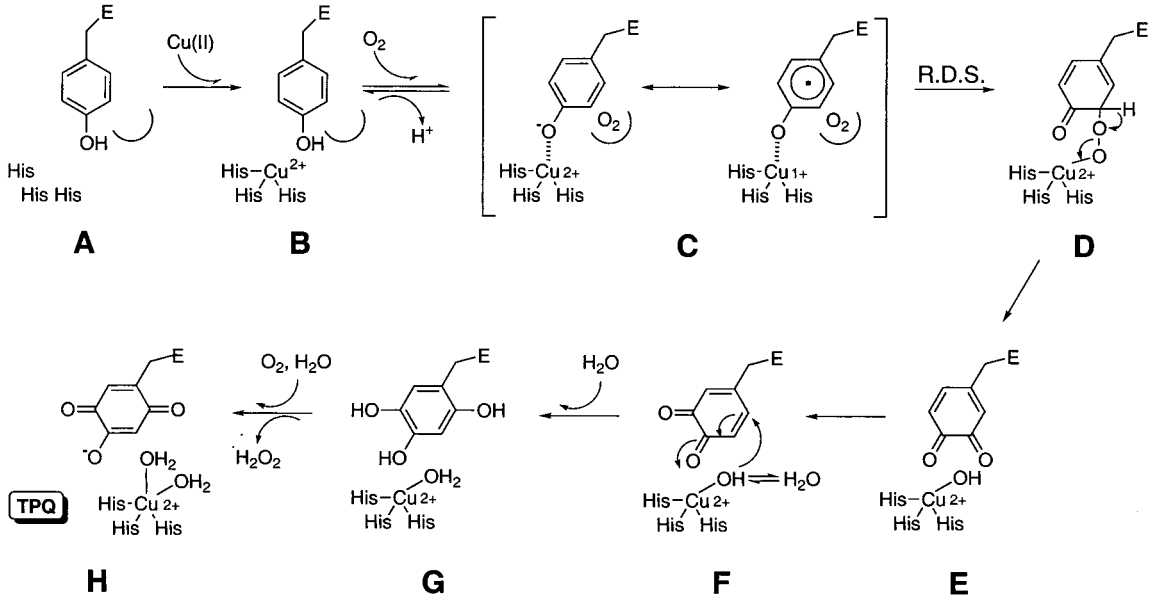

nonmetal site (*22*, *23*). This proposal was based on the observation of an intermediate with the properties of a tyrosine to copper charge-transfer complex, which was formed upon addition of oxygen to apo-Cu HPAO. However, further attempts to characterize this intermediate (such as resonance Raman spectroscopy) have been unsuccessful, and there still exists a fundamental lack of understanding in this area.

Early work in the amine oxidase field showed that azide can bind to copper in the mature protein (*26*, *27*); thus, N_3^- may be expected to be a good reporter for chemistry occurring at the active site metal in HPAO. Addition of azide to resting, mature HPAO resulted in an increase in absorbance at 408 nm (Figure 2A), and yielded a K_d of 55.5 mM (inset). This absorbance and binding affinity are similar to those noted for complex formation between N_3^- and Cu^{2+} in other amine oxidases, where it has been shown by EPR that azide displaces an equatorially liganded water (*27*, *30*). The effect of pH on the K_d for azide (Figure 2B) displays a pK_a of 7.6, quite close to that predicted for $Cu^{2+}-H_2O$ ionization (*34*), and inconsistent with ionization of azide itself [pK_a = 4.7 (*26*)].

Inhibition of HPAO by azide was studied in order to gauge the interaction between O_2 and the enzyme during the catalytic oxidative half-reaction. Azide is found to affect both k_{cat} and $k_{cat}/K_M(O_2)$ equally (Figure 3A,B). This behavior is concluded to result from noncompetitive inhibition and to be the result of the ability of both O_2 and N_3^- to bind to the same forms of the enzyme (*35*). It has been reported that reducing the mature enzyme diminishes the number of copper ligands from 5 to 4 (*6*), while the affinity of azide for the enzyme remains unchanged (*30*). The similar values and pH dependencies for the K_d (measured with oxidized enzyme) and the K_I (reflecting reduced enzyme) of azide (Figure 2B) support this conclusion. Thus, since only one site on the copper is expected to be available to exogenous ligand in reduced enzyme, these data are most easily reconciled with the binding of O_2 in a site off of the metal. This is consistent with the previously discussed proposals for O_2 binding in HPAO. Control experiments to account for the changing ionic strength, time-dependent binding of azide, and effects on K_M for amine cosubstrate were all performed, and found to not affect the results shown in Figure 3.

In contrast to the results found with HPAO, a similar study with an amine oxidase from porcine plasma (PPAO) reported that N_3^- displays competitive inhibition with respect to O_2 (*27*). Given the large degree of similarity among the active sites of all amine oxidases, it is tempting to assume that all CAOs should proceed through the same mechanism; in this case, the data for PPAO may reflect the inherent difficulty in distinguishing weak noncompetitive from competitive inhibition. However, it is important to note that differences do exist among amine oxidases. For example, the study in which the $Cu^{1+}-$TPQ semiquinone species was initially documented found that the accumulation of this species was highly dependent on the source of the amine oxidase (*18*). Thus, it is conceivable that different cofactor reoxidation mechanisms (Scheme 2A vs 2B) may occur, depending on the source of the enzyme.

As azide proved useful in studying catalysis, its effect on the biogenesis of TPQ in HPAO was also examined. Anaerobic titrations of apo-Cu HPAO displayed two distinct binding curves (Figure 4A,B). The first titration occurs with a K_d of 0.67 mM, and a λ_{max} = 412 nm ($\epsilon = 9.6 \times 10^2$ M^{-1} cm^{-1}). The second titration displayed a K_d of 21.1 mM, and a λ_{max} = 410 nm ($\epsilon = 6.3 \times 10^2$ M^{-1} cm^{-1}). The observation of two titratable positions on the copper is unexpected; in the structure of the zinc-containing apo-protein, the metal is tetrahedrally coordinated, with three histidines and the precursor tyrosine as ligands. However, the ability to access two sites on the copper argues that the geometry of apo-Cu HPAO may be closer to that found for oxidized, resting holoenzyme than the zinc enzyme.

The spectral course observed during biogenesis in the absence and presence of N_3^- is displayed in Figure 5A and Figure 5B, respectively. In the absence of azide, an intermediate transiently accumulates at 350 nm after the introduction of O_2, and subsequently decays concomitant with the production of TPQ (*22*). It has been previously argued that this corresponds to the formation and subsequent decay of a

Scheme 4: Previous (A) and New (B) Minimal Kinetic Models for Biogenesis

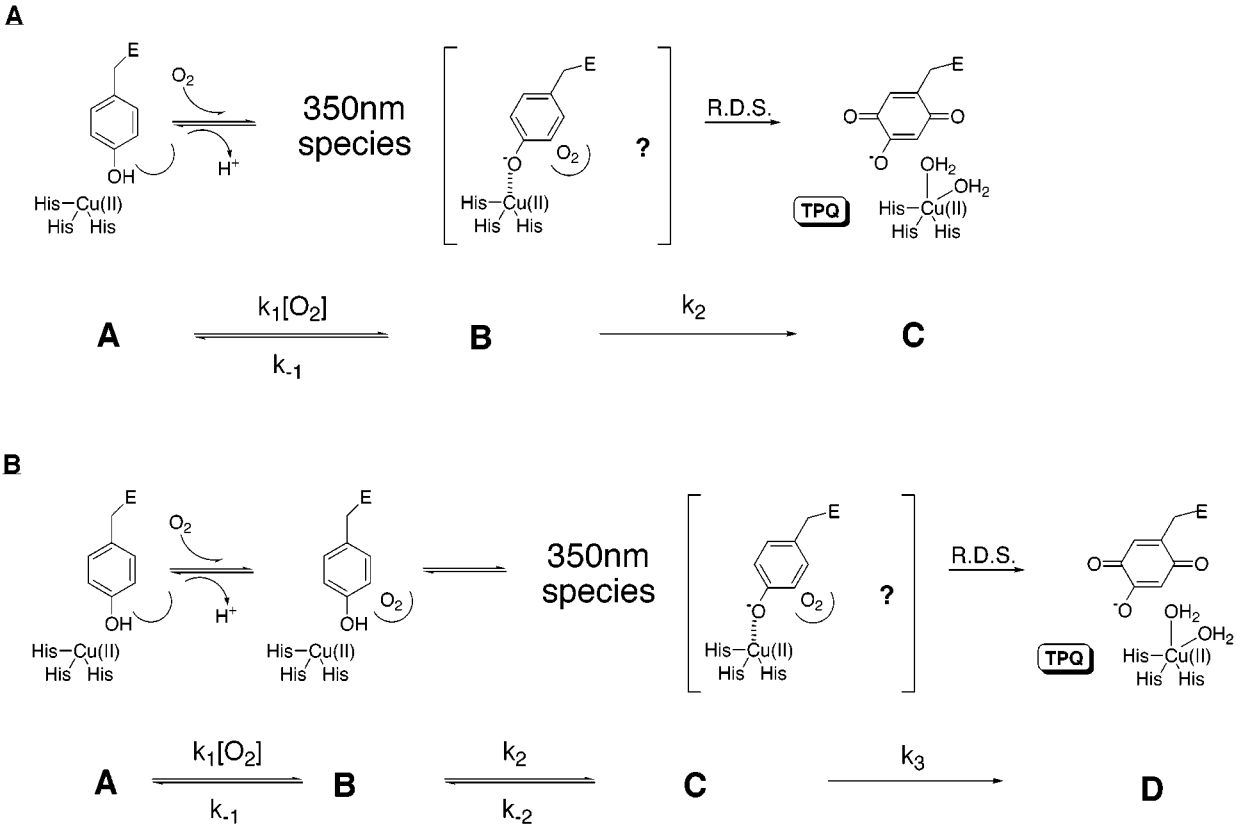

precursor tyrosine−copper complex, in a pseudoaxial orientation with respect to the metal (*8, 10, 22, 23*). In the presence of azide, anaerobic apo-Cu HPAO initially displays an absorbance corresponding to the $Cu^{2+}-N_3^-$ LMCT band at 410 nm; after the introduction of oxygen, this peak decays concomitantly with TPQ formation (Figure 5B). This result indicates that it is necessary to displace azide as a copper ligand during biogenesis. Based on the previous proposal for biogenesis (Scheme 3), it may be imagined that this could occur at several possible steps, by ligation of either the precursor tyrosine (B→C), the incipiently formed peroxo intermediate (C→D), or the water (G→H) to the copper.

To assess the inhibitory effect of azide on biogenesis, the observed rates of O_2 consumption and TPQ formation were measured as a function of azide concentration (Figure 7). Both rates are seen to decrease with increasing N_3^-, up to 10 mM. Previously, it was reported that in the absence of azide k_{obs} values for O_2 depletion and TPQ formation were quite similar (*22*); though that is found to be true here, the rates of the two processes become even closer as the concentration of azide increases. The previous kinetic model for biogenesis proposed a minimal two-step mechanism (A→B→C), whereby O_2 binding was coupled to formation of the observed intermediate, and was followed by decomposition to give TPQ (Scheme 4A). However, the different rates observed in Figure 7 are inconsistent with the earlier model in which the rates of both oxygen consumption and TPQ formation are determined by the slow equilibration of species B to C (*36*). Instead, it is necessary to add an additional kinetic step (A→B→C→D) between oxygen binding and TPQ formation to account for the data in Figure 7 (Scheme 4B). There are several important implications from this new model to be considered; first, it predicts that the decreased rate found as a function of azide concentration may be due to an effect on either k_1 or k_2; a decrease in k_3 would be expected to have a greater inhibitory effect on k_{obs} for TPQ formation than O_2 consumption. Second, the kinetic uncoupling of k_{obs} for these two observables should be detected by changes in other parameters, such as the concentration of O_2.

Each of the anticipated consequences of this new model can be tested experimentally. The first can be examined by observing the effect of increasing azide concentration on the 350 nm peak; it is expected that less of this species will accumulate if either the formation of the intermediate or the step preceding it is decreased. Indeed, at increasing concentrations of N_3^- (near the first K_d), the 350 nm peak visibly accumulates to a much smaller extent (Figure 6). The second expectation of this new model can be tested by observing the effect of varying the concentration of oxygen on k_{obs} for O_2 consumption and TPQ formation (Figure 8). As predicted, the two processes become kinetically uncoupled at elevated $[O_2]$, such that the rate for TPQ formation is observed to saturate, while that for oxygen consumption does not. This behavior can be understood by analyzing which rate constants contribute to the observed rates for the two processes.

The observed rate constants are composite values, consisting of contributions from the individual microscopic rates. Extensive treatment of these equations has been done by Bernasconi (*36*). Under the simplifying assumptions that in Scheme 4B $k_1[O_2]$, $k_{-1} > k_2$, $k_{-2} > k_3$, three separate composite rates may be coupled into the observed rates: a fast rate equal to $k_1[O_2] + k_{-1}$, an intermediate rate equal to $K_1[O_2]k_2/(1 + K_1[O_2]) + k_{-2}$ (where $K_1 = k_1/k_{-1}$), and a slow rate equal to $K_1[O_2]K_2k_3/(1 + K_1[O_2] + K_1[O_2]K_2)$ (where

Scheme 5: Mechanism for Biogenesis in the Presence of Azide

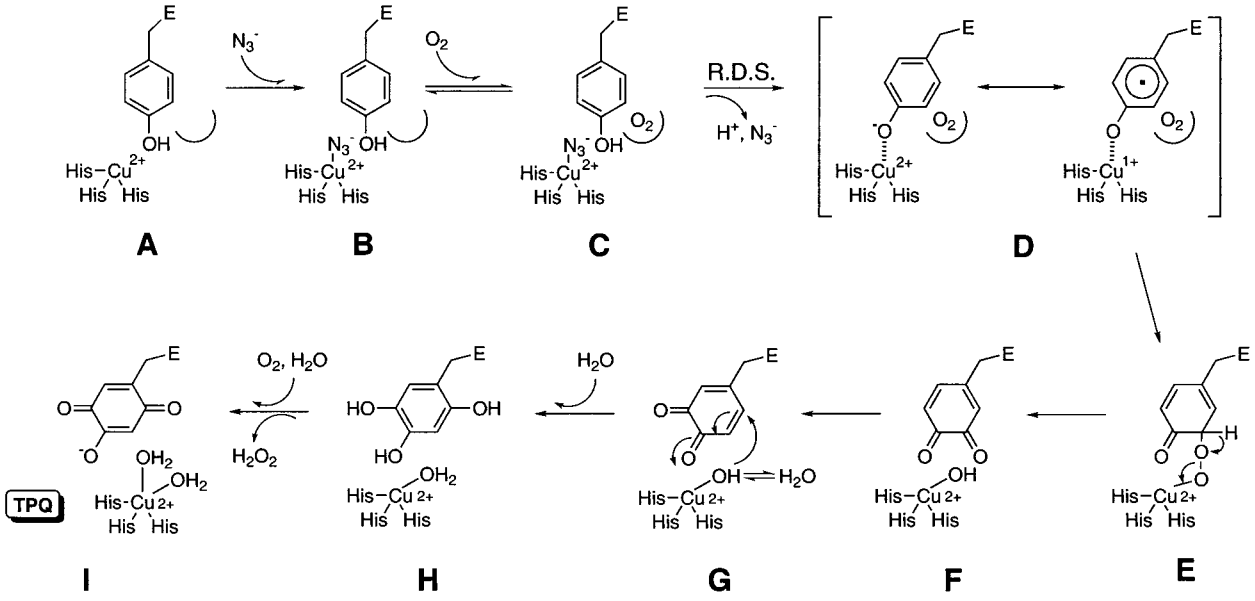

$K_2 = k_2/k_{-2}$). Each of these composite rates represents the equilibration through steps 1, 2, and 3 of the mechanism. For the experiments shown in Figure 8, enzyme was preequilibrated with oxygen, and biogenesis was initiated with copper; thus, the first equilibration in Scheme 4B will not be observed experimentally. While both the second and third equilibrations affect k_{obs} for $\Delta[O_2]$ and Δ[TPQ], they do so in different ways, leading to the observed variance in Figure 8. For $\Delta[O_2]$, steps 2 and 3 both contribute positively to the depletion of oxygen; thus, both factor into k_{obs}. However, for Δ[TPQ], only step 3 contributes to formation of cofactor; step 2 contributes a lag to these processes. Typically, the lag portion is short and not fit, and k_{obs} for TPQ will solely be a function of the composite rate for step 3. Thus, the uncoupling of rates observed in Figure 8 occurs because an increase in the concentration of oxygen leads to a proportionately smaller contribution of the third composite rate constant to the overall rate.

Though it is not possible to explicitly solve for all of the parameters in the second and third composite rate constants, several general conclusions can be drawn from Figure 8. As k_{obs} for TPQ saturates at a lower $[O_2]$ than does oxygen consumption, it follows that K_2 is large, while K_1 is relatively small. Using KINSIM, a reasonable set of parameters can be generated which reproduce all of the observed data: $K_1 = 1\ mM^{-1}$, $k_2 = 1\ min^{-1}$, $k_{-2} = 0.2\ min^{-1}$ ($K_2 = 5$), and $k_3 = 0.2\ min^{-1}$. We note that the fitted rate constants for k_2 and k_3 are ca. 2-fold larger than previous constants derived from a two-state model that lacks a step for O_2 binding prior to formation of the 350 nm species. This analysis helps to explain an apparent contradiction previously noted. While k_{obs} for O_2 depletion is not found to saturate up to 1 mM O_2, a large amount of the 350 nm intermediate could be observed spectroscopically under ambient conditions (*22*). This can be understood using the new model; if K_1 is small, K_2 is large, and $k_2 > k_3$, then the intermediate can accumulate to a significant extent.

As noted with the previous kinetic mechanism (*22*), the observed 350 nm intermediate is not necessarily confined to being the precursor tyrosine−copper complex. Indeed, any species shown in Scheme 3 which is present after O_2 is introduced (C to G) is conceivable. However, due to the observed spectral characteristics, several possibilities may logically be eliminated. Model compounds for dopa quinone (E) and reduced TPQ (G) have been synthesized, and display λ_{max} values in water of 400 and 300 nm, respectively; these are considered unlikely candidates for the observed intermediate (*37*, *38*). This leaves either the precursor tyrosine−copper species (C) or the peroxy intermediate (D), a possibility not previously entertained. No data are known for the peroxy species shown in Scheme 3, although Kitajima et al. (*41*) reported a λ_{max} close to 350 nm for a Cu^{2+}−peroxy adduct. However, several pieces of data support the 350 nm peak arising from species C. First, it has been observed that an increase in pH simultaneously increases the rate of biogenesis and the accumulation of the 350 nm intermediate (*23*). This seemingly contradictory result can be reconciled if the measured effects are ascribed to a tyrosine−copper LMCT species that ionizes in the experimental pH range. Second, a mutation of one of the copper ligands from His to Cys was found to shift the λ_{max} for the intermediate (*22*). This argues for significant electronic delocalization in the 350 nm species, easily understood for species C.

In total, the data suggest a mechanism for biogenesis in the presence of 1 bound equiv of azide (Scheme 5). Starting from anaerobic, copper-containing enzyme (A), the addition of azide leads to a 4-coordinate copper complex (B). While the observation of two binding sites for N_3^- in apo-Cu HPAO implies that both an axial site and an equatorial site are accessible (analogous to mature enzyme), the axial site is more likely the higher affinity site for the following reasons. First, the lower affinity site in apo-Cu HPAO has a binding constant similar to the single K_d found for mature enzyme, previously shown to be in the equatorial position. Second, it has been shown crystallographically for an analogue of apo-Cu HPAO containing zinc in the active site, that the precursor tyrosine ligands the metal in the axial position, while the equatorial site is unfilled (*10*). Thus, a clear mechanistic role for ligand affinity in the axial position is evident, whereas none is known for the equatorial one. Last,

a crystal structure of the reduced form of the mature enzyme trapped during turnover has implicated the axial site of the metal as the location of reduced O_2 during turnover (*6*). This predicted ligand preference is, however, different from that found for the resting, oxidized form of the enzyme (*29*). Thus, a detailed spectroscopic analysis of the apo-Cu protein with azide must be performed to decisively settle this issue.

With the introduction of oxygen to species B, O_2 binds weakly to a nonmetal site (C). Following this step, the precursor tyrosine must ligand the copper (D); however, the presence of azide slows down this step considerably, making it rate-determining. This mechanism is consistent with the observed spectral changes in Figure 5A and Figure 5B. In the absence of N_3^-, the rate-determining step is the breakdown of the 350 nm intermediate; thus, the decay of the 350 nm peak is isosbestic with TPQ formation. However, in the presence of azide, the rate-determining step is the formation of the intermediate. Its establishment requires the breakdown of the $Cu^{2+}-N_3^-$ complex and, thus, the observation of an isosbestic point between the decay of the 410 nm peak and formation of TPQ. This mechanism also accounts for the diminished observation of the 350 nm intermediate (Figure 6) in the presence of N_3^-. After formation of the intermediate (D), all steps may occur as previously imagined to lead to TPQ (I) and are expected to be relatively rapid.

Though this scenario appears most probable in explaining the effects of azide during biogenesis, in the above discussion we have also considered the possibility that the 350 nm species is not the precursor tyrosine. If it were the peroxo intermediate (E) of Scheme 5, the rate of cofactor biogenesis could still be limited by loss of N_3^- from the copper site. Ongoing spectroscopic efforts on the characterization of biogenetic intermediates should prove invaluable in confirming the proposed roles of oxygen and azide during biogenesis.

Not explored herein are the possible effects of the second equivalent of azide, which is inferred to bind in the mechanistically undefined equatorial position. It may be possible that this site normally interacts with oxygen or water. Future work will attempt to mitigate the effects of photodamage at high concentrations of azide in order to study this phenomenon.

CONCLUSIONS

Azide has been used as a general probe for understanding how oxygen interacts with HPAO. During catalysis, N_3^- binds to the active site copper and acts as a noncompetitive inhibitor with respect to O_2, consistent with previous conclusions that oxygen is bound off of the metal.

The presence of azide during biogenesis acts as an inhibitor, likely due to the need for the precursor tyrosine to ligand the active site copper. This proposal is consistent with the picture of biogenesis emerging from recent crystallographic, kinetic, and spectroscopic studies.

An intriguing feature of amine oxidases is that they are capable of catalyzing two different reactions within a single active site. Any particular mechanistic detail of these enzymes which is investigated may be considered within the context of this duality, because CAOs need to balance carefully the requirements of each transformation within the protein matrix. For example, studies of the conserved amino acids flanking TPQ (or the precursor tyrosine in apo-enzyme) have shown that these residues play largely conformational roles. During catalysis, mutation of these amino acids leads to accumulation of intermediates, while during biogenesis the precursor tyrosine is less able to access the copper (*14*, *22*, *23*, *39*, *40*). The inhibition of both processes by azide should also be considered in this fashion. It has been previously argued that the presence of copper during biogenesis is more crucial than during catalysis; indeed, no metal has been found to substitute for copper in cofactor formation, while other metals support turnover (*3*, *25*, *31*). The results of the azide inhibition support this analysis. The finding of two open binding sites on the metal in apo-protein supports the proposal that both the precursor tyrosine and an oxygenated intermediate need access to the metal during biogenesis. In the case of the holo-enzyme, only a single ligand site exists for N_3^-, consistent with the sole requirement of the metal to stabilize a reduced oxygen intermediate during catalysis.

ACKNOWLEDGMENT

We thank Joanne Dove for her invaluable help in understanding the single-turnover kinetics of biogenesis, and professor Frank Raushel (Texas A&M University) for providing the SGI version of KINSIM.

REFERENCES

1. Janes, S. M., Mu, D., Wemmer, D., Smith, A. J., Kaur, S., Maltby, D., Burlingame, A. L., and Klinman, J. P. (1990) *Science 248*, 981−987.
2. Mu, D., Janes, S. M., Smith, A. J., Brown, D. E., Dooley, D. M., and Klinman, J. P. (1992) *J. Biol. Chem. 267* (12), 7979−7982.
3. Matsuzaki, R., Fukui, T., Sato, H., Ozaki, Y., and Tanizawa, K. (1994) *FEBS Lett. 351*, 360−364.
4. Cai, D., and Klinman, J. P. (1994) *Biochemistry 33*, 7647−7653.
5. Parsons, M. R., Convery, M. A., Wilmot, C. M., Yadav, K. D. S., Blakeley, V., Corner, A. S., Phillips, S. E. V., McPherson, M. J., and Knowles, P. F. (1995) *Structure 3*, 1171−1184.
6. Wilmot, C. M., Hajdu, J., McPherson, M. J., Knowles, P. F., and Phillips, S. E. V. (1999) *Science 286*, 1724−1728.
7. Kumar, V., Dooley, D. M., Freeman, H. C., Guss, J. M., Harvey, I., McGuirl, M. A., Wilce, M. C. J., and Zubak, V. M. (1996) *Structure 4*, 943−955.
8. Wilce, M. C. J., Dooley, D. M., Freeman, H. C., Guss, J. M., Matsunami, H., McIntire, W. S., Ruggiero, C. E., Tanizawa, K., and Yamaguchi, H. (1997) *Biochemistry 36*, 16116−16133.
9. Li, R., Klinman, J. P., and Matthews, F. S. (1998) *Structure 6*, 293−307.
10. Chen, Z., Schwartz, B., Williams, N. K., Li, R., Klinman, J. P., and Mathews, F. S. (2000) *Biochemistry 39*, 9709−9717.
11. Wilmot, C. M., Murray, J. M., Alton, G., Parsons, M. R., Convery, M. A., Blakeley, V., Corner, A. S., Palcic, M. M., Knowles, P. F., McPherson, M. J., and Phillips, S. E. V. (1997) *Biochemistry 36*, 1608−1620.
12. Hartmann, C., and Klinman, J. P. (1987) *J. Biol. Chem. 262*, 962−965.
13. Hartmann, C., Brzovic, P., and Klinman, J. P. (1993) *Biochemistry 32*, 2234−2241.
14. Cai, D., Dove, J., Nakamura, N., Sanders-Loehr, J., and Klinman, J. P. (1997) *Biochemistry 36*, 11472−11478.
15. Nakamura, N., Moenne-Loccoz, P., Tanizawa, K., Mure, M., Suzuki, S., Klinman, J. P., and Sanders-Loehr, J. P. (1997) *Biochemistry 36*, 11479−11486.
16. Su, Q., and Klinman, J. P. (1998) *Biochemistry 37*, 12513−12525.

17. Hevel, J. M., Mills, S. A., and Klinman, J. P. (1999) *Biochemistry 38*, 3683−3693.
18. Dooley, D. M., McGuirl, M. A., Brown, D. E., Turowski, P. N., McIntire, W. S., and Knowles, P. F. (1991) *Nature 349*, 262−264.
19. Dooley, D. M., Scott, R. A., Knowles, P. F., Colangelo, C. M., McGuirl, M. A., and Brown, D. E. (1998) *J. Am. Chem. Soc. 120*, 2599−2605.
20. Nakamura, N., Matsuzaki, R., Choi, Y.-H., Tanizawa, K., and Sanders-Loehr, J. (1996) *J. Biol. Chem. 271* (9), 4718−4724.
21. Ruggiero, C. E., Smith, J. A., Tanizawa, K., and Dooley, D. M. (1997) *Biochemistry 36*, 1953−1959.
22. Dove, J. E., Schwartz, B., Williams, N. K., and Klinman, J. P. (2000) *Biochemistry 39*, 3690−3698.
23. Schwartz, B., Dove, J. E., and Klinman, J. P. (2000) *Biochemistry 39*, 3699−3707.
24. Turowski, P. N., McGuirl, M. A., and Dooley, D. M. (1993) *J. Biol. Chem. 268*, 17680−17682.
25. Mills, S. A., and Klinman, J. P. (2000) *J. Am. Chem. Soc. 122*, 9897−9904.
26. Olsson, B., Olsson, J., and Pettersson, G. (1978) *Eur. J. Biochem. 87*, 1−8.
27. Barker, R., Boden, N., Cayley, G., Charlton, S. C., Henson, R., Holmes, M. C., Kelly, I. D., and Knowles, P. F. (1979) *Biochem. J. 177*, 289−302.
28. Dooley, D. M., and Golnik, K. C. (1983) *J. Biol. Chem. 258*, 4245−4248.
29. Dooley, D. M., Cote, C. E., and Golnik, K. C. (1984) *J. Mol. Catal. 23*, 243−253.
30. McGuirl, M. A., Brown, D. E., and Dooley, D. M. (1997) *JBIC, J. Biol. Inorg. Chem. 2*, 336−342.
31. Cai, D., Williams, N. K., and Klinman, J. P. (1997) *J. Biol. Chem. 272*, 19277−19281.
32. Cleland, W. W. (1979) *Methods Enzymol. 63*, 103−138.
33. McIntire, W. S., and Hartmann, C. (1993) in *Principles and Applications of Quinoproteins* (Davidson, V. L., Ed.) pp 97−172, Marcel Dekker, Inc., New York.
34. Vatsimirksii, K. B., and Vasil'ev, V. P. (1960) in *Instability Constants of Complex Compounds*, pp 113−114, Pergamon Elmsford, New York.
35. Segel, I. H. (1993) in *Enzyme Kinetics. Behavior and Analysis of Rapid Equilibrium and Steady-State Enzyme Systems*, pp 125−136, John Wiley & Sons, Inc., New York.
36. Bernasconi, C. F. (1976) in *Relaxation Kinetics*, Academic Press, New York.
37. Mure, M., personal communication.
38. Mure, M., and Klinman, J. P. (1993) *J. Am. Chem. Soc. 115*, 7117−7127.
39. Schwartz, B., Green, E. L., Sanders-Loehr, J., and Klinman, J. P. (1998) *Biochemistry 37*, 16591−16600.
40. Choi, Y.-H., Matsuzaki, R., Suzuki, S., and Tanizawa, K. (1996) *J. Biol. Chem. 271*, 22598−22603.
41. Kitajima, N., Tsutomu, K., Fukjisawa, K., Iwata, Y., and Moro-aka, Y. (1993) *J. Am. Chem. Soc. 115*, 7872−7873.

BI0021378